

Molybdenum Nitrosyl Complexes and Their Application in Catalytic Imine Hydrogenation Reactions

Alexander Dybov,^[a] Olivier Blacque,^[a] and Heinz Berke^{*[a]}

Keywords: Molybdenum / Hydrogenation / Imines / Hydrides

The reaction between $[\text{Mo}(\text{CO})_4(\text{NO})(\text{ClAlCl}_3)]$ and the sterically hindered diphosphanes ($\text{P}(\text{NP})$ 1,3-bis(diisopropylphosphanyl)propane (dippp, **a**), 1,2-bis(diisopropylphosphanyl)ethane (dippe, **b**), 1,1'-bis(diisopropylphosphanyl)ferrocene (dippf, **c**) and 1,2-bis(dicyclohexylphosphanyl)ethane (dcype, **d**) produced the chlorides $[\text{Mo}(\text{P}(\text{NP})(\text{CO})_2(\text{NO})\text{Cl})]$ (**1a–1d**), which were transformed into the corresponding hydrides $[\text{Mo}(\text{P}(\text{NP})(\text{CO})_2(\text{NO})\text{H})]$ (**2a–2d**) by reaction with LiBH_4 in Et_3N at room temperature. The molybdenum–THF complex $[\text{Mo}(\text{dippp})(\text{CO})_2(\text{NO})(\text{THF})][\text{BAR}^{\text{F}}_4]$ [**3a**; $\text{Ar}^{\text{F}} = 3,5\text{-(CF}_3)_2\text{-C}_6\text{H}_3$], obtained by the reaction of **2a** with $[\text{H}(\text{Et}_2\text{O})_2][\text{BAR}^{\text{F}}_4]$, was exemplarily tested in the hydrogenation of the imine $\text{PhCH}=\text{N}(\alpha\text{-naphthyl})$. Replacement of the $[\text{BAR}^{\text{F}}_4]^-$ counter-

ion by the more stable $[\text{B}(\text{C}_6\text{F}_5)_4]^-$ anion greatly increased the catalytic activity. The use of in situ mixtures of the hydrides **2a–2d** and $[\text{H}(\text{Et}_2\text{O})_2][\text{B}(\text{C}_6\text{F}_5)_4]$ improved the hydrogenation activity. The hydride **2b** in combination with $[\text{H}(\text{Et}_2\text{O})_2][\text{B}(\text{C}_6\text{F}_5)_4]$ exhibited the highest TOF value of 123 h^{-1} in the reduction of $\text{PhCH}=\text{N}(\alpha\text{-naphthyl})$. The hydrogenation of the imines $\text{PhCH}=\text{NPh}$, $p\text{-ClC}_6\text{H}_4\text{CH}=\text{NPh}$, $p\text{-ClC}_6\text{H}_4\text{CH}=\text{N-}p\text{-C}_6\text{H}_4\text{Cl}$, $\text{PhCH}=\text{NCH}(\text{Ph})_2$ and $\text{PhCH}=\text{NMes}$ showed TOF values of 34, 74, 41, 18 and 84 h^{-1} at room temperature and a H_2 pressure of 30 bar. A mechanism for the ionic hydrogenation with “proton-before-hydride transfer” is anticipated.

Introduction

Homogeneous hydrogenation reactions are crucial in the production of numerous fine chemicals. Wilkinson- or Osborn-type catalysts^[1] are normally used in reactions involving the formal homolytic splitting of H_2 .^[2] These types of catalytic transformations are particularly suited to the hydrogenation of olefinic compounds. “Ionic hydrogenation”, operating by the heterolytic cleavage of H_2 , is largely a new approach.^[3,4] It involves the transfer of a hydride (H^-) or proton (H^+) as a H_2 equivalent to the substrate.^[5] Various catalytic systems enable the efficient hydrogenation of ketones^[6–8] and imines^[9–13] by Wilkinson/Osborn-type or ionic hydrogenation. However, most of these processes are presently based on precious metals, which require tedious catalyst recycling for economic and toxicity reasons. Therefore a global research approach has been initiated to develop non-precious metal catalysts.^[14,15] Bullock and co-workers reported some molybdenum and tungsten complexes $[\text{Cp}(\text{CO})_2\text{M}(\text{L})]^+[\text{A}]^-$ { $\text{M} = \text{Mo}, \text{W}$; $\text{L} = \text{phosphane}$, carbene; $\text{A} = \text{BAR}^{\text{F}}_4$ [$\text{Ar}^{\text{F}} = 3,5\text{-(CF}_3)_2\text{C}_6\text{H}_3$], $\text{B}(\text{C}_6\text{F}_5)_4$] that showed catalytic activity in ketone hydrogenation,^[16–20] but the TOF values achieved were still quite low. Mechan-

istic studies supported the “ionic hydrogenation” pathway with proton-before-hydride transfer.^[4] Furthermore, in related systems, Kubas and co-workers demonstrated the crucial influence of phosphane substitution on hydrogen activation through their electron-donating capability.^[21–24] For example, the complexes $[\text{Mo}(\text{CO})(i\text{Bu}_2\text{PCH}_2\text{CH}_2\text{P}i\text{Bu}_2)_2]$ bearing strong electron-donating ligands can split the H_2 molecule at ambient temperature to form a dihydride $\text{Mo}(\text{H})_2$ species, whereas the structurally similar $[\text{Mo}(\text{CO})(\text{Ph}_2\text{PCH}_2\text{CH}_2\text{PPh}_2)_2]$ complex coordinates the hydrogen molecule with an elongated H–H bond. In isoelectronic cationic bis(diphosphane)nitrosylmolybdenum and -tungsten complexes the H_2 ligand adds oxidatively to form dihydride complexes.^[25] H_2 complexes are normally more acidic than the corresponding dihydride complexes. Therefore the former species are preferably involved in heterolytic splitting by deprotonation and the latter foster catalyses of the Wilkinson type. The presence of nitrosyl ligands is expected to reduce the binding strength of H_2 ligands and enhance their acidity thus promoting the heterolytic splitting of H_2 .^[26,27] In addition we would expect for the deprotonated dihydrogen complexes the weakening of the resulting metal–hydride bonds to facilitate hydride transfers onto unsaturated compounds.^[28,29]

Based on this we supposed that (diphosphane)nitrosyl complexes of the type $[\text{Mo}(\text{NO})(\text{P}(\text{NP})(\text{CO})_2\text{L})][\text{A}]$ ($\text{L} = \text{labile ligand}$) might render catalytic ionic hydrogenation systems, particularly for imine hydrogenations with proton-before-hydride transfer characteristics.

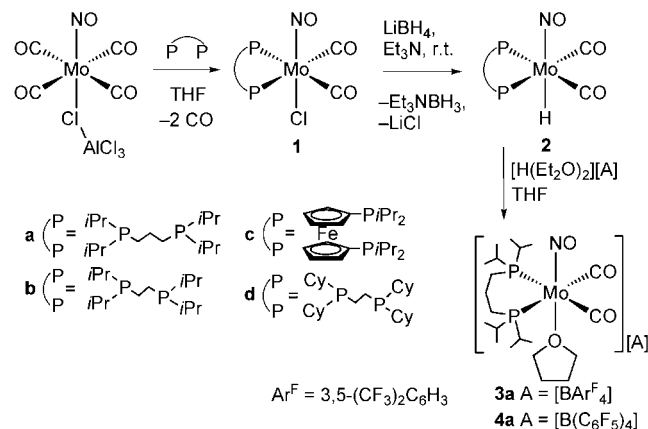
[a] Anorganisch-Chemisches Institut, Universität Zürich, Winterthurerstrasse 190, 8057 Zürich, Switzerland
Fax: +41-(0)44-635-68-03
E-mail: hberke@aci.uzh.ch

Supporting information for this article is available on the WWW under <http://dx.doi.org/10.1002/ejic.201000973>.

Results and Discussion

Synthesis and Characterization

The addition of 1 equiv. of the ligand dippp [dippp = 1,3-bis(diisopropylphosphanyl)propane] to a THF solution of $[\text{Mo}(\text{CO})_4(\text{NO})\text{ClAlCl}_3]$ revealed the formation of the chloride compound $[\text{Mo}(\text{dippp})(\text{NO})(\text{CO})_2(\text{Cl})]$ (**1a**; Scheme 1), which was isolated in 75% yield. The $^{31}\text{P}\{^1\text{H}\}$ NMR spectrum of **1a** exhibits a single resonance at $\delta = 21.5$ ppm, which indicates the presence of two equivalent phosphorus atoms. The ^1H NMR spectrum of **1a** shows two multiplets at $\delta = 2.36$ and 2.27 ppm, attributed to the $-\text{CH}$ protons of the isopropyl groups. In the $^{13}\text{C}\{^1\text{H}\}$ NMR spectrum the characteristic signal of the CO ligands appears as a doublet of doublets at $\delta = 215.9$ ppm ($^2J_{\text{CP}} = 22.9$ Hz). The IR spectrum reveals strong bands at 2019, 1950 $[\nu(\text{CO})]$ and 1610 cm^{-1} $[\nu(\text{NO})]$. X-ray diffraction studies of **1a** confirmed the spectroscopically derived pseudo-octahedral structures. An ORTEP drawing of **1a** is presented in Figure 1.



Scheme 1.

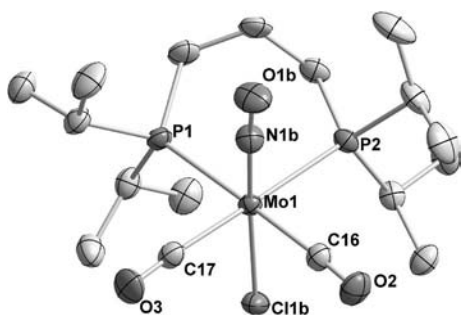


Figure 1. ORTEP drawing of $[\text{Mo}(\text{dippp})(\text{NO})(\text{CO})_2(\text{Cl})]$ (**1a**). Displacement ellipsoids are drawn at the 50% probability level. All hydrogen atoms and the positional disorder of NO and Cl have been omitted for clarity. Selected bond lengths [Å] and angles [°] for **1a**: Mo1–P1 2.5576(4), Mo1–P2 2.5780(5), Mo1–C17 2.043(2), Mo1–C16 2.034(2), C17–O3 1.130(2), C16–O2 1.134(2), N1b–O1b 1.218(12), P1–Mo1–P2 90.13(1), C17–Mo1–C16 89.75(7).

The crystal structure of **1a** reveals a disorder between the Cl atom and the *trans*-nitrosyl group. The phosphorus atoms and the two carbon atoms of the carbonyl groups

are in-plane with the metal. The average Mo–P bond length is 2.5678(5) Å.

Treatment of the chloride **1a** with 5 equiv. of LiBH_4 in Et_3N at room temperature resulted in the formation of the hydride complex **2a** (Scheme 1).^[25] The $^{31}\text{P}\{^1\text{H}\}$ NMR spectrum of **2a** exhibits a singlet at $\delta = 41.1$ ppm, which indicates the equivalence of the phosphane coordination. In addition to multiplets attributed to the resonance of the dippp protons, a characteristic triplet for the hydride ligand is observed in the ^1H NMR spectrum at -2.28 ppm ($^2J_{\text{PH}} = 24.0$ Hz). In the $^{13}\text{C}\{^1\text{H}\}$ NMR spectrum of **2a** the doublet of doublets at $\delta = 226.0$ ppm ($^2J_{\text{CP}} = 10.7$ Hz) has been attributed to the carbonyl ligands. The IR spectrum of **2a** reveals strong bands at 1983, 1910 $[\nu(\text{CO})]$, 1653 $[\nu(\text{MoH})]$ and 1570 $[\nu(\text{NO})]$ cm^{-1} .

An X-ray diffraction study was carried out on **2a** (Figure 2). Similar to the chloride compound **1a**, the hydride complex **2a** displays a pseudo-octahedral coordination geometry with the phosphorus atoms of the dippp ligand and the two carbonyl ligands in-plane with the metal centre and the hydride ligand located *trans* to the nitrosyl group. Structurally related bond lengths of **2a** are similar to those of the chloride **1a**.

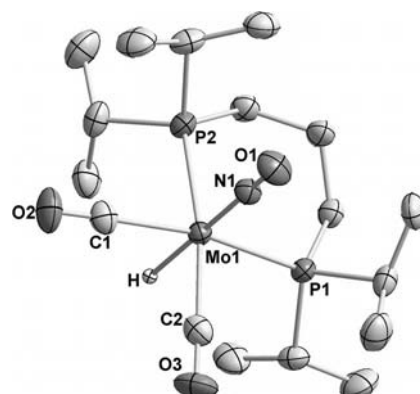


Figure 2. ORTEP drawing of $[\text{Mo}(\text{dippp})(\text{NO})(\text{CO})_2(\text{H})]$ (**2a**). Displacement ellipsoids are drawn at the 50% probability level. Selected hydrogen atoms have been omitted for clarity. Selected bond lengths [Å] and angles [°] for **2a**: Mo1–N1 1.829(2), Mo1–P1 2.5569(6), Mo1–P2 2.5347(7), Mo1–C1 2.017(3), Mo1–C2 2.018(3), Mo1–H 1.66(3), C1–O2 1.136(4), C2–O3 1.136(4), N1–O1 1.190(3), P1–Mo1–P2 90.3(2), C1–Mo1–C2 88.1(1).

Treatment of **2a** with 1 equiv. of $[\text{H}(\text{Et}_2\text{O})_2][\text{BAr}^{\text{F}}_4]$ ^[30–32] $[\text{Ar}^{\text{F}} = 3,5-(\text{CF}_3)_2\text{C}_6\text{H}_3]$ in THF afforded $[\text{Mo}(\text{dippp})(\text{NO})(\text{CO})_2(\text{THF})][\text{BAr}^{\text{F}}_4]$ (**3a**; Scheme 1), which was isolated in 69% yield. The $^{31}\text{P}\{^1\text{H}\}$ NMR spectrum of **3a** shows a singlet at $\delta = 17.6$ ppm. In the ^1H NMR spectrum characteristic multiplet resonances of THF appear at $\delta = 3.62$ and 1.78 ppm with the integration value correlating to integrations of the dippp ligand signals. The $^{13}\text{C}\{^1\text{H}\}$ NMR spectrum reveals a carbonyl resonance at $\delta = 214.1$ ppm ($^2J_{\text{CP}} = 16.7$ Hz) and the IR spectrum of **3a** shows strong bands at 2044, 1978 $[\nu(\text{CO})]$ and 1682 $[\nu(\text{NO})]$ cm^{-1} .

The X-ray diffraction studies of **3a** (Figure 3) showed a structure with pseudo-octahedral coordination of the metal centre similar to the hydride and chloride complexes **1a** and

2a with the two phosphorus atoms of the dippp ligands and the carbonyl ligands in-plane with the metal centre. The average M–P bond length of 2.588(2) Å is slightly longer than the corresponding bond lengths in **2a**. The THF molecule is coordinated to the metal centre with a M–O bond length of 2.241(4) Å. In the related complex $[(\mu\text{-H})\text{W}_2(\text{CO})_7(\text{THF})_2(\text{NO})]^{[33]}$ one THF molecule is also located *trans* to the nitrosyl ligand.

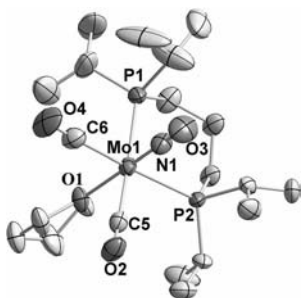


Figure 3. ORTEP drawing of $[\text{Mo}(\text{dippp})(\text{NO})(\text{CO})_2(\text{THF})][\text{BArF}_4]$ (**3a**). Displacement ellipsoids are drawn at the 50% probability level. Only the main residues (without counterion and free solvent molecules) are shown. Hydrogen atoms have been omitted for clarity. Selected bond lengths [Å] and angles [°] for **5a**: Mo1–N1 1.780(6), Mo1–P1 2.582(2), Mo1–P2 2.5840(15), Mo1–O1 2.241(4), Mo1–C6 2.053(8), Mo1–C5 2.060(7), C6–O4 1.12(1), C5–O2 1.12(1), N1–O3 1.188(7), P1–Mo1–P2 88.40(5), C1–Mo1–C2 87.6(3), O1–Mo1–N1 173.3(3).

The reaction of **2a** with $[\text{H}(\text{Et}_2\text{O})_2][\text{B}(\text{C}_6\text{F}_5)_4]$ produced the cationic complex $[\text{Mo}(\text{dippp})(\text{NO})(\text{CO})_2(\text{THF})][\text{B}(\text{C}_6\text{F}_5)_4]$ (**4a**). The $^{31}\text{P}\{\text{H}\}$ NMR spectrum exhibits a singlet resonance at $\delta = 16.5$ ppm for the dippp ligand. The $^{13}\text{C}\{\text{H}\}$ NMR spectrum shows a doublet of doublets at $\delta = 214.0$ ppm ($^2J_{\text{CP}} = 22.1$ Hz) attributed to the carbonyl ligands. The IR spectrum of **4a** displays two strong $\nu(\text{CO})$ bands at 2038 and 1970 cm^{-1} and a $\nu(\text{NO})$ band at 1668 cm^{-1} . However, the elemental analysis did not match the expected values presumably due to the fact that **4a** is an oil and could not be isolated in crystalline form. We supposed that the substance contained an excess of THF, which could not be removed in vacuo and prevented **4a** from crystallization.

A study of the influence of phosphane ligands on the reactivity of the complexes was attempted by the preparation of a series of molybdenum hydrides with different phosphane ligands (Scheme 1). The chlorides **1b–1d** were prepared by the reaction of $[\text{Mo}(\text{CO})_4(\text{NO})\text{ClAlCl}_3]$ with the diphosphane ligands 1,2-bis(diisopropylphosphanyl)ethane (dippe, **b**), 1,1'-bis(diisopropylphosphanyl)ferrocene (dippf, **c**) and 1,2-bis(dicyclohexylphosphanyl)ethane (dcype, **d**) in THF at room temperature. Then the chlorides were treated with excess LiBH_4 in Et_3N to afford the hydride complexes **2b–2d**. The NMR and IR spectra reveal the close structural relationships between **1b–1d** and **1a** and between **2b–2d** and **2a**. The spectroscopic data for compounds **1** and **2** are summarized in Table 1.

Table 1. Selected spectroscopic data for **1a–d** and **2a–d**.

	$\delta(\text{MoP})$ [ppm]	$\delta(\text{MoH})$ [ppm]	$\delta(\text{CO})$ [ppm]	IR vibration frequency [cm^{-1}]		
				$\nu(\text{CO})$	$\nu(\text{MH})$	$\nu(\text{NO})$
1a	21.5		215.9	2019	1950	1610
1b	61.1		217.1	2020	1949	1611
1c	29.8		216.5	2021	1950	1610
1d	53.5		217.4	2022	1948	1614
2a	41.1	–2.28	226.0	1983	1910	1653
2b	84.5	–3.44	226.8	1983	1910	1653
2c	48.3	–1.20	226.2	1981	1902	1637
2d	53.5	–3.25	227.1	1986	1920	1647

Complexes **1d** and **2b** were additionally characterized by X-ray diffraction analyses. The ORTEP drawings of **1d** and **2b** are shown in Figure 4. Similarly to **1a** the structure of **1d** displays a pseudo-octahedral coordination geometry with two phosphane atoms and two carbonyls in-plane with the molybdenum centre. The asymmetric unit of **1d** contains one half of the molecule as the metal centre lies on a crystallographic two-fold axis. Consequently, the *trans* Cl and NO ligands are positionally disordered with an occupancy ratio of 0.5. The Mo–P bond length is 2.5319(7) Å, which is slightly shorter than the corresponding mean value of **1a**, presumably due to the smaller bite angle of the dcype ligand in comparison with the dippp derivative.^[34] A similar tendency can be observed on comparing the bond lengths of **2a** and **2b**. The mean Mo–P bond length in **2b** is 2.513 Å, whereas the mean Mo–P bond length in **2a** was found to be 2.546 Å. The Mo–H bond is rather long [1.83(4) Å], which indicates the suitability of such a complex for hydride transfer processes.

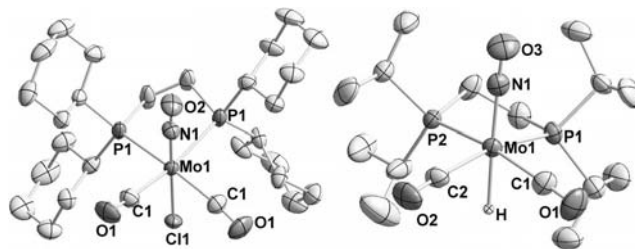


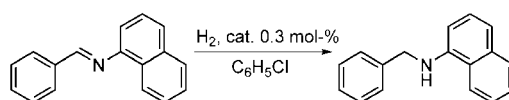
Figure 4. ORTEP drawings of $[\text{Mo}(\text{dcype})(\text{NO})(\text{CO})_2(\text{Cl})]$ (**1d**) and $[\text{Mo}(\text{dippe})(\text{NO})(\text{CO})_2(\text{H})]$ (**2b**). Displacement ellipsoids are drawn at the 50% probability level. Selected hydrogen atoms and the positional disorder of NO and Cl in **1d** have been omitted for clarity. Selected bond lengths [Å] and angles [°] for **1d**: Mo1–N1 1.772(5), Mo1–P1 2.5319(7), Mo1–Cl1 2.517(3), Mo1–C1 2.043(2), C1–O1 1.135(4), N1–O2 1.195(6) Cl1B–Mo1–N1B 179.4(2), P1–Mo1–P1 81.23(2), C1–Mo1–C1 89.0(1). Selected bond lengths [Å] and angles [°] for **2b**: Mo1–N1 1.868(3), Mo1–P1 2.5054(8), Mo1–P2 2.5205(8), Mo1–H 1.83(4), Mo1–C1 2.007(3), Mo1–C2 2.023(3), C1–O1 1.148(7), C2–O2 1.137(4), N1–O3 1.152(4), P1–Mo1–P2 80.26(3), C1–Mo1–C2 90.1(1).

Imine Hydrogenation

Complex **3a** was first tested as a catalyst in the hydrogenation of the imine $\text{PhCH}=\text{N}(\alpha\text{-naphthyl})$. The reaction was carried out at 10 bar H_2 and 80 °C in $\text{C}_6\text{H}_5\text{Cl}$.^[35] However,

only 5% conversion of the imine was observed (Table 2). A kinetic analysis demonstrated that the reaction proceeded well during the initial 30 min after which the catalyst decomposed presumably due to the limited stability of the $[\text{BAr}^{\text{F}}_4]^-$ counterion.^[36,37] We therefore looked for an alternative more stable counterion. The $[\text{B}(\text{C}_6\text{F}_5)_4]^-$ anion is known to display a lower coordination ability and higher stability towards fluorine abstraction than $[\text{BAr}^{\text{F}}_4]^-$.^[38]

Table 2. Catalytic hydrogenation of $\text{PhCH}=\text{N}(\alpha\text{-naphthyl})$.



Entry	Cat.	Pressure [bar]	Temp. [°C]	Initial TOF [h ⁻¹]	Conv. [%]	Reaction time [h]
1	3a	10	80	—	5	0.5
2	2a ^[a]	30	r.t.	106	>99	13
3	4a	30	r.t.	95	>99	14
4	2b ^[a]	30	r.t.	123	>99	11
5	2c ^[a]	30	r.t.	68	>99	16
6	2d ^[a]	30	r.t.	50	>99	19

[a] A mixture of the corresponding hydride and $[\text{H}(\text{Et}_2\text{O})_2][\text{B}(\text{C}_6\text{F}_5)_4]$ was used as a catalyst.

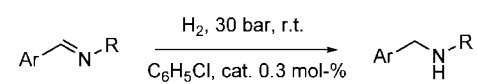
The use of **4a** as the catalyst in the imine hydrogenation of $\text{PhCH}=\text{N}(\alpha\text{-naphthyl})$ revealed 100% conversion of the substrate and a TOF value of 95 h⁻¹ in the first hour at room temperature under a H₂ pressure of 30 bar (Table 2). An increase in temperature led to significantly lower conversions, presumably due to the decomposition of the catalyst during catalysis. Note that no hydrogenation was observed when the reaction was conducted in THF as solvent. Moreover, more quantitative experiments, in which THF was initially added to the reaction mixture in various amounts, demonstrated an inverse dependence of the rate of hydrogenation on the amount of added THF. We supposed that THF acts as a ligand and thereby blocks catalytically crucial vacant sites of various intermediates and consequently reduces the catalytic turnover. Hydrogenation reactions without the involvement of THF were also realized by the direct use of the pure hydride **2a** and $[\text{H}(\text{Et}_2\text{O})_2][\text{B}(\text{C}_6\text{F}_5)_4]$ as a co-catalyst. Solutions of the substrate in C₆H₅Cl were added to this mixture and pressurized with 30 bar of H₂. This approach revealed a slightly higher rate of hydrogenation (TOF = 105 h⁻¹) than with pure **4a**.

To study the influence of the bite angle of the diphosphane ligands^[39] on the reactivity the hydrides **2b–2d** were also tested in the hydrogenation of $\text{PhCH}=\text{N}(\alpha\text{-naphthyl})$ (Table 2). The lowest rate of hydrogenation was found for **2d** (initial TOF = 50 h⁻¹), presumably due to the high steric congestion of the cyclohexyl substituent of the dcype ligand, which prevents a facile approach of the $\text{PhCH}=\text{N}(\alpha\text{-naphthyl})$ substrate to the metal centre. Complexes **2a–2c** showed a strong dependence of the diphosphane bite angle^[40] on the rate of hydrogenation. Complex **2c** with the largest bite angle in this series demonstrated the lowest activity (initial TOF = 68 h⁻¹), whereas the hydrides **2a** and **2b**

exhibited significantly higher rates of hydrogenation (initial TOF values: 106 h⁻¹ for **2a**, 123 h⁻¹ for **2b**). Most likely, the shorter bridge “pulls” the sterically demanding isopropyl group to one side opening up another side of the molecule to allow the substrate enter.

The hydride **2b** showed the best catalytic performance of all the experiments with $\text{PhCH}=\text{N}(\alpha\text{-naphthyl})$ and was therefore used in the hydrogenation of other imines. The results of these catalytic experiments are presented in Table 3.

Table 3. Catalytic hydrogenation of imines with **2b** as catalyst.

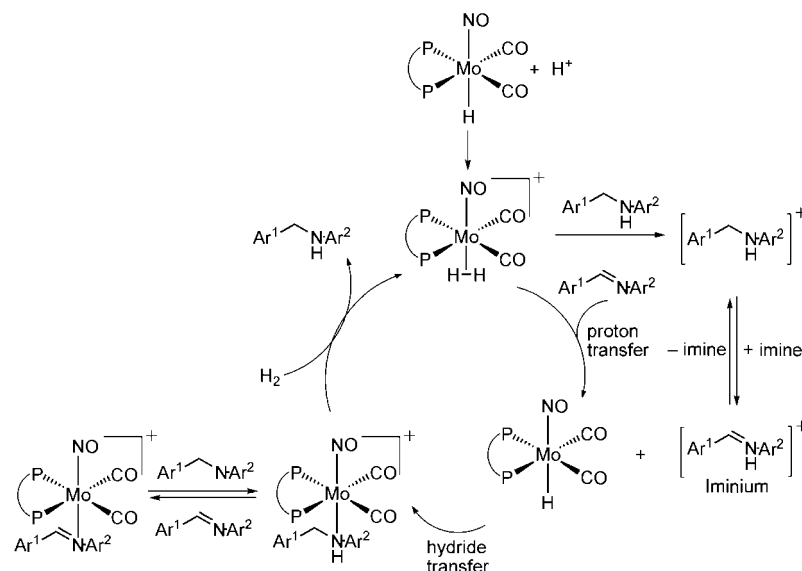


cat. = **2b** + $[\text{H}(\text{Et}_2\text{O})_2][\text{B}(\text{C}_6\text{F}_5)_4]$

Entry	Substrate	TOF [h ⁻¹]	Conv. [%]	Reaction time [h]
1	$\text{PhCH}=\text{N}(\alpha\text{-naphthyl})$	123	>99	11
2	$\text{PhCH}=\text{NPh}$	34	80	24
3	$p\text{-ClC}_6\text{H}_4\text{CH}=\text{NPh}$	74	96	16
4	$p\text{-ClC}_6\text{H}_4\text{CH}=\text{N-}p\text{-C}_6\text{H}_4\text{Cl}$	41	66	17
5	$\text{PhCH}=\text{NCHPh}_2$	18	45	35
6	$\text{PhCH}=\text{NMe}_3$	84	>99	20
7	$\text{PhCH}=\text{NiBu}$	—	≈0.3	—

A mechanism for the hydrogenation of imines with the Mo catalysts is presented in Scheme 2. The initial protonation of the hydride results in a short-lived dihydrogen complex,^[41] which is the key species that drives the catalytic cycle. An iminium salt might then be formed by proton transfer from the acidic dihydrogen complex.^[4,13] To validate the iminium as a key intermediate in the hydrogenation, a reduction was carried out in which a catalytic amount of separately obtained iminium salt and **2b** were used. This experiment did not reveal any significant difference in the rate of hydrogenation and conversion compared with the result described above (Table 2, entry 1). Both the imine and amine product are expected to be involved in a protolytic equilibrium, which would require that the electrophilic iminium as a reactant is present in sufficient concentration that subsequent hydride transfer could become kinetically feasible. The deprotonation of the dihydrogen ligand comprises the heterolytic splitting of H₂ and this presumably is the rate-limiting step. The highest rates of hydrogenation were observed with more bulky substrates (entries 1 and 6, Table 3), which apparently facilitate the amine dissociation from the molybdenum centre required for re-entry of H₂ into the cycle. Amine, imine and H₂ coordination have to be considered competitive.

Crucial to the course of the hydrogenation reaction is the formation of the iminium cation, which competes with the formation of the ammonium salt produced from the protonation of the amine products. All imine/amine pairs with aryl substituents generally showed low basicities, but the imine is the stronger base. Conversely, the basicities of alkyl-substituted imine/amine are generally higher with the



Scheme 2. Mechanism of imine hydrogenation following a proton-before-hydride transfer scheme.

amine more basic than the corresponding imine derivatives. Thus, we anticipated that the hydrogenation of aniline derivatives could be readily accomplished because their imines are stronger bases than the amines and the iminium cation should therefore be available in kinetically relevant concentrations. In the case of alkylimine derivatives (entries 5 and 7, Table 3) we could not achieve satisfactory conversions probably due to the fact that the amine is the stronger base and would consume a significant proportion of the protons thus blocking their involvement in the catalytic cycle. The alkylamines would also be stronger ligands and could block the metal centre if not enough protons can be supplied to scavenge the amine as an ammonium salt. In the case of *N*-alkyl-substituted $\text{PhCH}=\text{NCHPh}_2$, the basicities of the amine and the imine are presumably comparable and the reaction was found to stop when a certain amount of amine is produced, which would be in accord with the given rationalization of the protolytic equilibrium.

The difference in $\text{p}K_{\text{b}}$ of the $\text{PhCH}=\text{N}i\text{Bu}/\text{PhCH}_2\text{NH}i\text{Bu}$ pair seems to be so high that only the amine is expected to be present in the protonated form. Indeed, the rate of hydrogenation of this compound was zero. Presumably the low yield of the reaction of entry 4 of Table 3 with a chlorine-containing substrate can be related to a blocking of the molybdenum centre with chloride released during catalysis.^[42]

Conclusions

A series of hydride complexes of the type $[\text{Mo}(\text{P}(\text{ONP})_2(\text{CO})_2(\text{NO})\text{H}]$ bearing bulky diphosphane ligands have been prepared by the reaction of $[\text{Mo}(\text{P}(\text{ONP})_2(\text{CO})_2(\text{NO})\text{Cl}]$ with LiBH_4 in Et_3N at room temperature. In combination with $[\text{H}(\text{Et}_2\text{O})_2][\text{B}(\text{C}_6\text{F}_5)_4]$ the hydrides showed valuable catalytic activity in the hydrogenation of the imine $\text{PhCH}=\text{N}(\alpha\text{-naphthyl})$. The widely used $[\text{BAr}^{\text{F}}_4]^-$ counterion apparently

is too unstable under the conditions employed in the imine hydrogenations. In contrast, in the presence of the $[\text{B}(\text{C}_6\text{F}_5)_4]^-$ anion the reactive $16e^-$ molybdenum centre possesses enough stability and flexibility to promote the proper exchanges of weak ligands. The complex $[\text{Mo}(\text{dippe})(\text{CO})_2(\text{NO})\text{H}]$ (**2b**) displayed the best activity with an initial TOF of 123 h^{-1} in the hydrogenation of $\text{PhCH}=\text{N}(\alpha\text{-naphthyl})$. This hydride was also tested as a catalyst to hydrogenate various other aryl imines. The hydrogenation of alkyl imines was found to be inferior to aryl imines. All these observations can be explained on the basis of an “ionic hydrogenation” pathway occurring with heterolytic cleavage of H_2 and “proton-before-hydride” transfer.

Experimental Section

General: Reagent-grade benzene, toluene, pentane, diethyl ether and tetrahydrofuran were dried and distilled from sodium benzophenone ketyl prior to use. Acetone and CH_2Cl_2 were dried with CaH_2 and then distilled. Literature procedures were used to prepare the following compounds: 1,3-bis(diisopropylphosphanyl)propane (dipp),^[43] 1,2-bis(diisopropylphosphanyl)ethane (dippe), 1,2-bis(dicyclohexylphosphanyl)ethane (dcype),^[44] 1,1'-bis(diphenylphosphanyl)ferrocene (dippf),^[45] $[\text{H}(\text{Et}_2\text{O})_2][\text{BAr}^{\text{F}}_4]$,^[46] $[\text{H}(\text{Et}_2\text{O})_2][\text{B}(\text{C}_6\text{F}_5)_4]$,^[38] and $[\text{Mo}(\text{CO})_4(\text{NO})(\text{ClAlCl}_3)]$.^[47] Other reagents were purchased and used without further purification. All the manipulations were carried out under nitrogen using Schlenk techniques or in a dry glovebox. IR spectra were obtained with a Bio-Rad FTS-45 instrument. NMR spectra were recorded with Varian Mercury 200 (200.1 MHz for ^1H , 81.0 MHz for $^{31}\text{P}\{^1\text{H}\}$), Bruker DRX 500 (500.2 MHz for ^1H , 202.5 MHz for $^{31}\text{P}\{^1\text{H}\}$, 125.8 MHz for $^{13}\text{C}\{^1\text{H}\}$) and Bruker DRX 400 spectrometers (400.1 MHz for ^1H , 162.0 MHz for $^{31}\text{P}\{^1\text{H}\}$, 100.6 MHz for $^{13}\text{C}\{^1\text{H}\}$). Chemical shifts in ^1H and $^{13}\text{C}\{^1\text{H}\}$ NMR spectra are given in ppm relative to TMS (SiMe_4), the resonances in the $^{31}\text{P}\{^1\text{H}\}$ NMR spectra are referenced to 98% external H_3PO_4 . Elemental analyses were performed with a Leco CHN(S)-932 instrument. The hydrogen pressure in the catalytic reactions was monitored with “WIKA” Transmitter CPT

2500 instrument. The GC–MS spectra were recorded with a Varian Saturn 2000 spectrometer equipped with a Varian 450-GC chromatograph. Gas flow: 1.0 mL/min. Temperature regime: 70 °C, 0.5 min hold, then 20 °C/min. The following column was used: VF-5ms 30.0 m × 0.25 mm, ID = 0.25 mm.

General Procedure for the Synthesis of the Diphosphane-Substituted Complexes [Mo(PNP)(CO)₂(NO)Cl] (1a–1d): A solution of the diphosphane ligand (1.0 mmol) in THF (10 mL) was added to a solution of [Mo(CO)₄(NO)ClAlCl₃] (1.0 mmol) in THF (15 mL). The reaction mixture was stirred for 10 h at room temperature. Then the solvent was removed in vacuo. The residue was extracted with Et₂O until the extracted solution became colourless. The combined Et₂O fractions were concentrated to the half of their original volume and cooled to –30 °C. The precipitate formed was filtered off and dried in vacuo.

[Mo(dippf)(CO)₂(NO)Cl] (1a): Yield 75%, 372.2 mg. ¹H NMR (400.1 MHz, CD₂Cl₂, 25 °C): δ = 2.36 [m, 2 H, PCH(CH₃)₂], 2.27 [m, 2 H, PCH(CH₃)₂], 2.12 (m, 4 H, PCH₂CH₂CH₂P), 1.90 (m, 8 H, PCH₂CH₂CH₂P), set of multiplets from 1.33 to 1.25 (24 H, CH₃) ppm. ³¹P{¹H} NMR (162.0 MHz, CD₂Cl₂, 25 °C): δ = 21.5 (s) ppm. ¹³C{¹H} NMR (100.6 MHz, CD₂Cl₂, 25 °C): δ = 215.9 (dd, ²J_{CP} = 38.2, ²J_{CP} = 22.7 Hz, CO), 27.4 [m, PCH(CH₃)₂], 26.6 [m, PCH(CH₃)₂], 21.9 (m, PCH₂CH₂CH₂P), 20.0 (m, PCH₂CH₂CH₂P), 19.9 (s, CH₃), 19.7 (s, CH₃), 19.1 (s, CH₃) ppm. IR (ATR): ν̃ = 2019, 1950 (CO) 1610 (NO) cm^{–1}. C₁₇H₃₄ClMoNO₃P₂ (493.8): calcd. C 41.35, H 6.94, N 2.84; found C 41.08, H 7.04, N 2.69.

[Mo(dippe)(CO)₂(NO)Cl] (1b): Yield 43%, 205.9 mg. ¹H NMR (400.1 MHz, CD₂Cl₂, 25 °C): δ = 2.41 [m, 2 H, PCH(CH₃)₂], 2.30 [m, 2 H, PCH(CH₃)₂], 1.94 (m, 4 H, PCH₂CH₂P), set of multiplets from 1.37 to 1.23 (24 H, CH₃) ppm. ³¹P{¹H} NMR (162.0 MHz, CD₂Cl₂, 25 °C): δ = 61.1 (s) ppm. ¹³C{¹H} NMR (100.6 MHz, CD₂Cl₂, 25 °C): δ = 217.0 (dd, ²J_{CP} = 51.3, ²J_{CP} = 10.7 Hz, CO), 25.6 [m, PCH(CH₃)₂], 24.0 [m, PCH(CH₃)₂], 22.9 (dd, ¹J_{CP} = 17.9, ¹J_{CP} = 14.3 Hz, PCH₂CH₂P), 20.5 (s, CH₃), 20.3 (s, CH₃), 20.2 (s, CH₃), 18.6 (s, CH₃) ppm. IR (ATR): ν̃ = 2020, 1949 (CO), 1611 (NO) cm^{–1}. C₁₆H₃₂ClMoNO₃P₂ (479.8): calcd. C 40.05, H 6.72, N 2.92; found C 40.21, H 6.63, N 2.81.

[Mo(dippf)(CO)₂Cl] (1c): Yield 64%, 406.8 mg. ¹H NMR (400.1 MHz, CD₂Cl₂, 25 °C): δ = 4.56 (s, 2 H, Cp), 4.45 (s, 2 H, Cp), 4.44 (s, 2 H, Cp), 4.41 (s, 2 H, Cp), 2.55 [m, 4 H, PCH(CH₃)₂], set of multiplets from 1.55 to 1.23 (24 H, CH₃) ppm. ³¹P{¹H} NMR (162.0 MHz, CD₂Cl₂, 25 °C): δ = 29.8 (s) ppm. ¹³C{¹H} NMR (100.6 MHz, CD₂Cl₂, 25 °C): δ = 216.5 (dd, ²J_{CP} = 61.2, ²J_{CP} = 18.1 Hz, CO), 76.4 [m, PC(CH)₂(CH)₂], 75.6 [t, ²J_{CP} = 5.0 Hz, PC(CH)₂(CH)₂], 75.3 [t, ²J_{CP} = 4.0 Hz, PC(CH)₂(CH)₂], 71.7 [t, ²J_{CP} = 2.0 Hz, PC(CH)₂(CH)₂], 71.4 [t, ²J_{CP} = 2.0 Hz, PC(CH)₂(CH)₂], 29.2 [t, ¹J_{CP} = 8.03 Hz, PCH(CH₃)₂], 28.7 [t, ¹J_{CP} = 9.0 Hz, PCH(CH₃)₂], 20.9 (s, CH₃), 20.5 (s, CH₃), 19.8 (s, CH₃), 18.8 (s, CH₃) ppm. IR (ATR): ν̃ = 2021, 1950 (CO), 1610 (NO) cm^{–1}. C₂₄H₃₆ClFeMoNO₃P₂ (635.7): calcd. C 45.34, H 5.71, N 2.20; found C 45.23, H 5.80, N 2.15.

[Mo(dcyep)(CO)₂(NO)Cl] (1d): Yield 83%, 265.6 mg. ¹H NMR (500.2 MHz, CD₂Cl₂, 25 °C): set of multiplets from 2.2 to 1.1. ³¹P{¹H} NMR (202.5 MHz, CD₂Cl₂, 25 °C): δ = 53.5 (s) ppm. ¹³C{¹H} NMR (160.5 MHz, CD₂Cl₂, 25 °C): δ = 217.4 (dd, ²J_{CP} = 51.3, ²J_{CP} = 10.7 Hz, CO), 35.9 (m, PCH), 34.0 (m, PCH), 30.7 (s, Cy), 30.6 (s, Cy), 30.3 (s, Cy), 29.1 (s, Cy), 28.1 (m, Cy), 27.8 (m, Cy), 27.7 (m, Cy), 26.7 (s, Cy), 26.6 (s, Cy), 21.0 (dd, ¹J_{CP} = 17.9, ¹J_{CP} = 14.3 Hz, PCH₂CH₂P) ppm. IR (ATR): ν̃ = 2022, 1948 (CO), 1614 (NO) cm^{–1}. C₂₈H₄₈ClMoNO₃P₂ (640.0): calcd. C 52.54, H 7.56, N 2.19; found C 52.38, H 7.47, N 2.15.

General Procedure for the Synthesis of the Diphosphane-Substituted Hydrides [Mo(PNP)(CO)₂(NO)H] (2a–2d): Et₃N (10 mL) was added to a mixture of [Mo(PNP)(CO)₂(NO)Cl] (0.25 mmol) and LiBH₄ (27.5 mg, 1.25 mmol). The reaction mixture was stirred at room temperature until no trace of the starting material [monitoring with ³¹P{¹H} NMR] was observed (≈10 h). The Et₃N was removed in vacuo. The residue was extracted with benzene until the extracted solution became colourless. After removal of the benzene the residue was extracted again with hexane until the extracted solution became colourless. Then the combined hexane fractions were concentrated to half of their original volume and cooled to –30 °C. The precipitate formed was filtered off and dried in vacuo.

[Mo(dippf)(CO)₂(NO)H] (2a). Yield 67%, 76.8 mg. ¹H NMR (400.1 MHz, C₆D₆, 25 °C): set of multiplets from 1.82 to 1.62 [4 H, PCH(CH₃)₂], set of multiplets from 1.62 to 1.28 (6 H, PCH₂CH₂CH₂P), set of multiplets from 1.15 to 0.79 (24 H, CH₃), –2.28 (t, ²J_{PH} = 24.0 Hz, 1 H, Mo–H) ppm. ³¹P{¹H} NMR (162.0 MHz, C₆D₆, 25 °C): δ = 41.1 (s) ppm. ¹³C{¹H} NMR (100.6 MHz, C₆D₆, 25 °C): δ = 226.0 (t, ²J_{CP} = 10.7 Hz, CO), 29.2 [t, ¹J_{CP} = 10.7 Hz, PCH(CH₃)₂], 27.6 [t, ¹J_{CP} = 13.1 Hz, PCH(CH₃)₂], 22.7 (t, ²J_{CP} = 4.8 Hz, PCH₂CH₂CH₂P), 20.0 (t, ¹J_{CP} = 9.5 Hz, PCH₂CH₂CH₂P), 19.6 (s, CH₃), 18.8 (s, CH₃), 18.8 (s, CH₃), 17.5 (s, CH₃) ppm. IR (ATR): ν̃ = 1983, 1910 (CO), 1653 (MoH), 1570 (NO) cm^{–1}. C₁₇H₃₅MoNO₃P₂ (459.4): calcd. C 44.45, H 7.68, N 3.05; found C 44.27, H 7.99, N 3.10.

[Mo(dippe)(CO)₂(NO)H] (2b): Yield 53%, 59.4 mg. ¹H NMR (400.1 MHz, C₆D₆, 25 °C): δ = 1.78 [m, 2 H, PCH(CH₃)₂], 1.67 [m, 2 H, PCH(CH₃)₂], 1.18 (m, 4 H, PCH₂CH₂P), set of multiplets from 1.09 to 0.81 (24 H, CH₃), 3.43 (t, ²J_{PH} = 26.3 Hz, 1 H, Mo–H) ppm. ³¹P{¹H} NMR (162.0 MHz, C₆D₆, 25 °C): δ = 84.5 (s) ppm. ¹³C{¹H} NMR (100.6 MHz, C₆D₆, 25 °C): δ = 226.8 (dd, ²J_{CP} = 33.4, ²J_{CP} = 10.7 Hz, CO), 28.3 [m, PCH(CH₃)₂], 26.7 [m, PCH(CH₃)₂], 22.5 (t, ¹J_{CP} = 15.5 Hz, PCH₂CH₂P), 19.7 (s, CH₃), 19.5 (s, CH₃), 19.3 (s, CH₃), 18.8 (s, CH₃) ppm. IR (ATR): ν̃ = 1983, 1910 (CO), 1653 (MoH), 1570 (NO) cm^{–1}. C₁₆H₃₃MoNO₃P₂ (445.3): calcd. C 43.15, H 7.47, N 3.15; found C 42.71, H 7.79, N 3.18.

[Mo(dippf)(CO)₂(NO)H] (2c): Yield 49%, 74.6 mg. ¹H NMR (400.1 MHz, C₆D₆, 25 °C): δ = 4.17 (s, 2 H, Cp), 4.03 (s, 2 H, Cp), 4.01 (s, 2 H, Cp), 3.98 (s, 2 H, Cp), 2.12 [m, 4 H, PCH(CH₃)₂], set of multiplets from 1.27 to 0.96 (24 H, CH₃), –1.20 (t, ²J_{PH} = 23.6 Hz, 1 H, Mo–H) ppm. ³¹P{¹H} NMR (162.0 MHz, C₆D₆, 25 °C): δ = 48.2 (s) ppm. ¹³C{¹H} NMR (100.6 MHz, C₆D₆, 25 °C): δ = 226.2 (dd, ²J_{CP} = 38.1, ²J_{CP} = 11.0 Hz, CO), 76.9 [m, PC(CH)₂(CH)₂], 75.3 [t, ²J_{CP} = 4.0 Hz, PC(CH)₂(CH)₂], 74.9 [t, ²J_{CP} = 4.0 Hz, PC(CH)₂(CH)₂], 71.0 [t, ²J_{CP} = 2.0 Hz, PC(CH)₂(CH)₂], 70.9 [t, ²J_{CP} = 2.0 Hz, PC(CH)₂(CH)₂], 29.2 [dd, ¹J_{CP} = 11.0, ¹J_{CP} = 9.0 Hz, PCH(CH₃)₂], 26.5 [dd, ¹J_{CP} = 12.1, ¹J_{CP} = 10.0 Hz, PCH(CH₃)₂], 20.0 (s, CH₃), 19.8 (s, CH₃), 19.1 (s, CH₃), 19.1 (s, CH₃) ppm. IR (ATR): ν̃ = 1983, 1902 (CO), 1637 (MoH), 1574 (NO) cm^{–1}. C₂₄H₃₇FeMoNO₃P₂ (601.3): calcd. C 47.94, H 6.20, N 2.33; found C 47.80, H 6.11, N 2.27.

[Mo(dcyep)(CO)₂(NO)H] (2d): Yield 63%, 95.6 mg. ¹H NMR (400.1 MHz, C₆D₆, 25 °C): set of multiplets from 2.2 to 1.1, –3.25 (t, ²J_{PH} = 26.3 Hz, 1 H, Mo–H) ppm. ³¹P{¹H} NMR (162.0 MHz, C₆D₆, 25 °C): δ = 53.5 (s) ppm. ¹³C{¹H} NMR (100.6 MHz, C₆D₆, 25 °C): δ = 227.1 (dd, ²J_{CP} = 32.2, ²J_{CP} = 10.7 Hz, CO), 38.0 (m, PCH), 37.0 (m, PCH), 29.9 (s, Cy), 29.8 (s, Cy), 29.2 (s, Cy), 28.9 (s, Cy), 27.8 (m, Cy), 26.8 (s, Cy), 26.6 (s, Cy), 22.6 (dd, ¹J_{CP} = 17.6, ¹J_{CP} = 15.5 Hz, PCH₂CH₂P) ppm. IR (ATR): ν̃ = 1986, 1920 (CO), 1647 (MoH), 1574 (NO) cm^{–1}. C₂₈H₄₉MoNO₃P₂ (605.6): calcd. C 55.53, H 8.16, N 2.31; found C 55.17, H 8.34, N 2.26.

Synthesis of [Mo(dipp)(CO)₂(NO)(THF)][BAR^F₄] (3a): A solution of [H(Et₂O)₂][BAR^F₄] (43.8 mg, 0.043 mmol) in THF (2 mL) was slowly added to a solution of [Mo(dipp)(CO)₂(NO)H] (20.0 mg, 0.043 mmol) in THF (2 mL) at room temperature. The reaction mixture was stirred for 2 h. Then the solvent was evaporated in vacuo. Hexane (2 mL) was added to the residue and then the Et₂O was added dropwise to the suspension until the solid was completely dissolved. The solution was cooled to −30 °C to afford a precipitate of **3a** that was filtered and dried in vacuo. Yield 69%, 41.4 mg. ¹H NMR (400.1 MHz, [D₈]THF, 25 °C): δ = 7.79 (s, 8 H, *o*-Ph), 7.57 (s, 4 H, *p*-Ph), 3.62 (m, 4 H, THF), 2.48 [m, 4 H, PCH(CH₃)₂], 2.23 (m, 4 H, PCH₂CH₂CH₂P), 1.91 (m, 2 H, PCH₂CH₂CH₂P), 1.77 (m, 4 H, THF), set of multiplets from 1.39 to 1.28 (24 H, CH₃) ppm. ³¹P{¹H} NMR (162.0 MHz, [D₈]THF, 25 °C): δ = 17.7 (s) ppm. ¹³C{¹H} NMR (100.6 MHz, [D₈]THF, 25 °C): δ = 214.1 (dd, ²J_{CP} = 32.2, ²J_{CP} = 16.7 Hz, CO), 163.0 (q, ¹J_{BC} = 50.0 Hz, *i*-BAR^F₄), 135.8 (s, *o*-BAR^F₄), 130.1 (m, *m*-BAR^F₄), 125.5 (q, ¹J_{CF} = 273.4 Hz, CF₃), 118.4 (s, *p*-BAR^F₄), 68.2 (s, THF), 27.9 [m, PCH(CH₃)₂], 26.4 (s, THF), 22.5 (t, ²J_{CP} = 8.3 Hz, PCH₂CH₂CH₂P), 20.4 (s, CH₃), 20.1 (s, PCH₂CH₂CH₂P), 19.4 (s, CH₃), 19.1 (s, CH₃), 18.7 (s, CH₃) ppm. IR (ATR): ν̃ = 2044, 1978 (CO), 1682 (NO) cm^{−1}. C₅₃H₅₄BF₂₄MoNO₄P₂ (1393.7): calcd. C 45.68, H 3.91, N 1.01; found C 45.61, H 3.78, N 1.00.

Synthesis of [Mo(dipp)(CO)₂(NO)(THF)][B(C₆F₅)₄] (4a): A solution of [H(Et₂O)₂][B(C₆F₅)₄] (37.1 mg, 0.043 mmol) in THF (2 mL) was slowly added to a solution of [Mo(NO)(dipp)(CO)₂H] (20.0 mg, 0.043 mmol) in THF (2 mL) at room temperature. The reaction mixture was stirred for 2 h. Then the solvent was evaporated in vacuo to afford an oil that was used without further purification. ¹H NMR (400.1 MHz, [D₈]THF, 25 °C): δ = 3.37 (m, 4 H, THF), 2.59 [m, 4 H, PCH(CH₃)₂], 2.23 (m, 4 H, PCH₂CH₂CH₂P), 1.91 (m, 2 H, PCH₂CH₂CH₂P), 1.77 (m, 4 H, THF), set of multiplets from 1.38 to 1.28 (24 H, CH₃) ppm. ³¹P{¹H} NMR (162.0 MHz, [D₈]THF, 25 °C): δ = 16.5 (s) ppm. ¹³C{¹H} NMR (125.8 MHz, [D₈]THF, 25 °C): δ = 214.0 (dd, ²J_{CP} = 32.1, ²J_{CP} = 22.1 Hz, CO), 149.0 (br. d, ¹J_{CF} = 235.9 Hz, *o*-C₆F₅), 139.1 (dm, ¹J_{CF} = 242.1 Hz, *p*-C₆F₅), 137.0 (dm, ¹J_{CF} = 244.1 Hz, *m*-C₆F₅), 125.7 (br. m, *i*-C₆F₅), 68.10 (s, THF), 28.0 [m, PCH(CH₃)₂], 26.0 (s, THF), 22.6 (t, ²J_{CP} = 8.0 Hz, PCH₂CH₂CH₂P), 20.5 (s, CH₃), 20.2 (s, PCH₂CH₂CH₂P), 19.5 (s, CH₃), 19.2 (s, CH₃), 18.8 (s, CH₃) ppm. IR (ATR): ν̃ = 2038, 1970 (CO), 1668 (NO) cm^{−1}. The elemental analysis did not match the theoretical values due to presence of THF in a non-stoichiometric ratio.

General Procedure for the Catalytic Experiments: A solution of the substrate (2.0 mmol) in C₆H₅Cl (5 mL) was added to a mixture of the [Mo(P(ΠP)(CO)₂(NO)H] catalyst (0.006 mmol, 0.3 mol-%) and [H(Et₂O)₂][B(C₆F₅)₄] (5.0 mg, 0.006 mmol). The mixture was placed in an autoclave and pressurized with 30 bar H₂. The H₂ pressure was monitored by a precision pressure probe. When the pressure changes were approaching zero, the reaction mixture was removed from the autoclave and filtered through silica gel. Without any further purification, a GC–MS spectrum was recorded to determine the conversion of the hydrogenation reaction and identify the products. PhCH=N(*α*-naphthyl): *t*_R = 10.532 min, *m/z* = 231; PhCH₂NH(*α*-naphthyl): *t*_R = 10.607 min, *m/z* = 233; PhCH=NPh: *t*_R = 7.460 min, *m/z* = 181; PhCH₂NHPh: *t*_R = 7.695 min, *m/z* = 183; *p*-ClC₆H₄CH=NPh: *t*_R = 8.636 min, *m/z* = 215; *p*-ClC₆H₄CH₂NHPh: *t*_R = 8.989 min, *m/z* = 217; *p*-ClC₆H₄CH=N-*p*-C₆H₄Cl: *t*_R = 9.639 min, *m/z* = 249; *p*-ClC₆H₄CH₂NH-*p*-C₆H₄Cl: *t*_R = 10.114 min, *m/z* = 251; PhCH=NCHPh₂: *t*_R = 10.589 min, *m/z* = 271; PhCH₂NHCHPh₂: *t*_R = 10.386 min, *m/z* = 273; PhCH=NMe: *t*_R = 8.301 min, *m/z* = 223; PhCH₂NHMe: *t*_R =

8.491 min, *m/z* = 225; PhCH=NiBu: *t*_R = 4.876 min, *m/z* = 161; PhCH₂NHiBu: *t*_R = 5.756 min, *m/z* = 163.

X-ray Diffraction Studies of 1a, 1d, 2a, 2b and 3a: Relevant details regarding the structural refinements are given in Tables S1 and S2 of the Supporting Information and selected geometrical parameters are included in the captions of the corresponding figures. Intensity data were collected at 183(2) K with an Oxford Xcalibur diffractometer (4-circle kappa platform, Ruby CCD detector and a single wavelength Enhance X-ray source with Mo-*K*_α radiation, λ = 0.71073 Å).^[48] Suitable selected single crystals were mounted using polybutene oil on the top of a glass fibre fixed on a goniometer head and immediately transferred to the diffractometer. Pre-experiment, data collection, data reduction and absorption corrections were performed with CrysAlisPro.^[48] The crystal structures were solved with SHELXS-97^[49] using direct methods. The structure refinements were performed by full-matrix least-squares methods on *F*² with SHELXL-97.^[49] PLATON^[50] was used to check the results of the X-ray analyses. All programs used during the crystal structure determination process are included in the WINGX software.^[51] The hydride atoms were located in difference Fourier maps and all other hydrogen atoms were placed at ideal positions and refined with fixed isotropic displacement parameters using a riding model.

CCDC-791648 (for **1a**), -791649 (for **1d**), -791650 (for **2a**), -791651 (for **2b**) and -791652 (for **3a**) contain the supplementary crystallographic data for this paper. These data can be obtained free of charge from The Cambridge Crystallographic Data Centre via www.ccdc.cam.ac.uk/data_request/cif.

Supporting Information (see footnote on the first page of this article): X-ray crystallographic data for all determined molecular structures.

Acknowledgments

We thank the University of Zürich and the Swiss National Science Foundation for financial support.

- [1] J. A. Osborn, F. H. Jardine, J. F. Young, G. I. Wilkinson, *J. Chem. Soc.* **1966**, 1711–1732.
- [2] P. A. Chaloner, M. A. Esteruelas, F. Jos, L. A. Oro, *Homogeneous Hydrogenation*, Kluwer, Dordrecht, **1994**.
- [3] D. N. Kursanov, Z. N. Parnes, N. M. Loim, *Synthesis* **1974**, 633–651.
- [4] H. Berke, *ChemPhysChem* **2010**, *11*, 1837–1849.
- [5] R. M. Bullock, *Chem. Eur. J.* **2004**, *10*, 2366–2374.
- [6] R. Noyori, *Angew. Chem. Int. Ed.* **2002**, *41*, 2008–2022.
- [7] P. J. Fagan, M. H. Voges, R. M. Bullock, *Organometallics* **2010**, *29*, 1045–1048.
- [8] M. A. Esteruelas, C. Garcia-Yebra, E. Onate, *Organometallics* **2008**, *27*, 3029–3036.
- [9] H. R. Guan, M. Iimura, M. P. Magee, J. R. Norton, G. Zhu, *J. Am. Chem. Soc.* **2005**, *127*, 7805–7814.
- [10] C. P. Casey, G. A. Bikzhanova, I. A. Guzei, *J. Am. Chem. Soc.* **2006**, *128*, 2286–2293.
- [11] M. P. Magee, J. R. Norton, *J. Am. Chem. Soc.* **2001**, *123*, 1778–1779.
- [12] G. Hou, F. Gosselin, W. Li, C. McWilliams, Y. K. Sun, M. Weisel, P. D. O'Shea, C. Y. Chen, I. W. Davies, X. M. Zhang, *J. Am. Chem. Soc.* **2009**, *131*, 9882–9883.
- [13] X. Y. Liu, K. Venkatesan, H. W. Schmalle, H. Berke, *Organometallics* **2004**, *23*, 3153–3163.
- [14] M. R. Bullock, *Handbook of Homogeneous Hydrogenation*, Wiley-VCH, Weinheim, **2007**.
- [15] R. M. Bullock, *Angew. Chem. Int. Ed.* **2007**, *46*, 7360–7363.

- [16] M. R. Bullock, M. H. Voges, *J. Am. Chem. Soc.* **2000**, *122*, 12594–12595.
- [17] M. H. Voges, R. M. Bullock, *J. Chem. Soc., Dalton Trans.* **2002**, 759–770.
- [18] B. F. M. Kimmich, P. J. Fagan, E. Hauptman, R. M. Bullock, *Chem. Commun.* **2004**, 1014–1015.
- [19] B. F. M. Kimmich, P. J. Fagan, E. Hauptman, W. J. Marshall, R. M. Bullock, *Organometallics* **2005**, *24*, 6220–6229.
- [20] F. Wu, V. K. Dioumaev, D. J. Szalda, J. Hanson, R. M. Bullock, *Organometallics* **2007**, *26*, 5079–5090.
- [21] G. J. Kubas, R. R. Ryan, D. A. Wroblewski, *J. Am. Chem. Soc.* **1986**, *108*, 1339–1341.
- [22] G. J. Kubas, C. J. Unkefer, B. I. Swanson, E. Fukushima, *J. Am. Chem. Soc.* **1986**, *108*, 7000–7009.
- [23] H. J. Wasserman, G. J. Kubas, R. R. Ryan, *J. Am. Chem. Soc.* **1986**, *108*, 2294–2301.
- [24] G. J. Kubas, R. R. Ryan, C. J. Unkefer, *J. Am. Chem. Soc.* **1987**, *109*, 8113–8115.
- [25] A. Dybov, O. Blacque, H. Berke, *Eur. J. Inorg. Chem.* **2010**, 3328–3337.
- [26] N. Avramovic, J. Höck, O. Blacque, T. Fox, H. W. Schmalle, H. Berke, *J. Organomet. Chem.* **2010**, *695*, 382–391.
- [27] J. Höck, H. Jacobsen, H. W. Schmalle, G. R. J. Artus, T. Fox, J. I. Amor, F. Bath, H. Berke, *Organometallics* **2001**, *20*, 1533–1544.
- [28] F. Liang, H. W. Schmalle, T. Fox, H. Berke, *Organometallics* **2003**, *22*, 3382–3393.
- [29] Z. Chen, H. W. Schmalle, T. Fox, H. Berke, *Dalton Trans.* **2005**, 580–587.
- [30] L. K. Johnson, C. M. Killian, M. Brookhart, *J. Am. Chem. Soc.* **1995**, *117*, 6414–6415.
- [31] J. Campora, J. A. Lopez, P. Palma, P. Valerga, E. Spillner, E. Carmona, *Angew. Chem. Int. Ed.* **1999**, *38*, 147–151.
- [32] R. A. Widenhoefer, A. Vadehra, P. K. Cheruvu, *Organometallics* **1999**, *18*, 4614–4618.
- [33] M. K. Lee, P. S. Huang, Y. S. Wen, J. T. Lin, *Organometallics* **1990**, *9*, 2181–2183.
- [34] C. A. Tolman, *Chem. Rev.* **1977**, *77*, 313–348.
- [35] Chlorobenzene was used as a non-coordinating polar solvent with a high boiling point. The catalyst is insoluble in the non-polar solvents benzene or toluene.
- [36] W. V. Konze, B. L. Scott, G. J. Kubas, *Chem. Commun.* **1999**, 1807–1808.
- [37] H. Salem, L. J. W. Shimon, G. Leitus, L. Weiner, D. Milstein, *Organometallics* **2008**, *27*, 2293–2299.
- [38] P. Jutzi, C. Müller, A. Stämmler, H. G. Stämmler, *Organometallics* **2000**, *19*, 1442–1444.
- [39] M. Kranenburg, Y. E. M. Vanderburgt, P. C. J. Kamer, P. W. N. M. Vanleeuwen, K. Goubitz, J. Fraanje, *Organometallics* **1995**, *14*, 3081–3089.
- [40] N. Fey, J. N. Harvey, G. C. Lloyd-Jones, P. Murray, A. G. Orpen, R. Osborne, M. Purdie, *Organometallics* **2008**, *27*, 1372–1383.
- [41] D. M. Heinekey, W. J. Oldham, *Chem. Rev.* **1993**, *93*, 913–926.
- [42] B. Lucht, M. J. Poss, T. G. Richmond, *J. Chem. Educ.* **1991**, *68*, 786–788.
- [43] E. Lindner, M. Schmid, J. Wald, J. A. Queisser, M. Geprags, P. Wegner, C. Nachtigal, *J. Organomet. Chem.* **2000**, *602*, 173–187.
- [44] R. J. Burt, J. Chatt, W. Hussain, G. J. Leigh, *J. Organomet. Chem.* **1979**, *182*, 203–206.
- [45] T. J. Kim, Y. H. Kim, Y. H. Kim, S. C. Shim, Y. W. Kwak, J. S. Cha, H. S. Lee, J. K. Uhm, S. I. Byun, *Bull. Korean Chem. Soc.* **1992**, *13*, 588–592.
- [46] M. Brookhart, B. Grant, A. F. Volpe, *Organometallics* **1992**, *11*, 3920–3922.
- [47] K. Seyferth, R. Taube, *J. Organomet. Chem.* **1982**, *229*, 275–279.
- [48] Xcalibur CCD System, CrysAlisPro software, versions 1.171.32.24–1.171.33.52, Oxford Diffraction Ltd., Abingdon, England, **2007**.
- [49] G. M. Sheldrick, *Acta Crystallogr., Sect. A* **2008**, *64*, 112–122.
- [50] A. L. Spek, *J. Appl. Crystallogr.* **2003**, *36*, 7–13.
- [51] L. J. Farrugia, *J. Appl. Crystallogr.* **1999**, *32*, 837–838.

Received: September 13, 2010

Published Online: December 29, 2010